Research Journal of Applied Sciences, Engineering and Technology 7(6): 1149-1155, 2014
DOI:10.19026/rjaset.7.373
ISSN: 2040-7459; e-ISSN: 2040-7467

Submitted: February 27, 2013 Accepted: March 27, 2013 Published: February 15, 2014

Research Article

Design of a Neural Controller for Single Phase Inverter in Grid Connected Photovoltaic System

[1]A. Ndiaye, [1]L. Thiaw, [1]G. Sow, [1]S.S. Fall, [1]M. Thiam, [1]M. Kassé and [2]G. Sissoko
[1]Laboratory of Renewable Energy, Polytechnic Higher School,
University Cheikh Anta Diop, Dakar-Fann, Senegal
[2]Laboratory of Semiconductors and Solar Energy, Physics Department, Faculty of
Science and Technology, University Cheikh Anta Diop, Dakar, Senegal

Abstract: This study shows a neural network based control strategy of the current injected into a single-phase grid via an inverter. The inverter is supplied by a Photovoltaic Generator (PVG). The optimal control of PVG is ensured by an MPPT algorithm of type P and O (Perturbation-Observation). The synchronization of the inverter with the electrical grid is ensured by a Phase-Locked Loop (PLL) device. The sizing and the modeling of the system components have been presented. A Neural Network Controller (NNC) and a Proportional Integral (PI) controller have been implemented and compared. Obtained results show that the NNC have faster response and lower THD without overshoots.

Keywords: Modeling, MPPT, neural network controller, proportional integral controller, single-phase inverter

INTRODUCTION

The main difficulties in the control strategy of real dynamic systems are the non-linearity and uncertainties. The control of the system requires in general the development of a mathematical model making it possible to establish the transfer function of the system that links the inputs and the outputs. This supposes good knowledge of the dynamic and properties of the system. In the non-linear system case, the conventional techniques have often shown their limits mainly when the system to be studied presents strong non-linearity. The lack of right knowledge necessary for the development of the mathematical models is somehow the origin of those limits (Mohammed *et al*., 2007).

Recourse to the control methods based on artificial intelligence has become a necessity. These control methods follow a process of extraction of the knowledge of the system to be studied from collected empirical data, so as to be able to react in front of new situations: this strategy is known as intelligent control (Panos and Kevin, 1993).

Artificial Neural Networks (ANN) are used in intelligent control due to the fact that they are parsimonious universal approximators (Panos and Kevin, 1993; Rivals *et al*., 1995) and that they have the capacity to adapt to a dynamic evolving through time. Moreover, as multi-input and multi-output systems, they can be used in the frame of the control of the multivariable systems.

A feed-forward ANN makes one or more algebraic functions of its inputs, by the composition of the functions made by each one of its neurons (Dreyfus, 2002). These are organized in layers and inter-connected by well-balanced synaptic connections. The supervised training of a neural network consists in modifying the weights to have a given behavior minimizing a cost function often represented by the quadratic-error (Panos and Kevin, 1993; Cybenko, 1989).

Several authors have tried to exploit the advantages of neural networks to control a dynamic system, precisely, within the field of robotics (Rivals *et al*., 1995; Yildirim, 1997) and for the control of asynchrony motors (Mohammed *et al*., 2007; Panos and Kevin, 1993; Branštetter and Skotnica, 2000). More details on neural network controllers can be found in Panos and Kevin (1993), Wishart and Harley (1995) and Ronco and Gawthrop (1997).

Tine *et al*. (2009) made a comparative study between PI controller, PID controller and a fuzzy logic based controller for an inverter control shows that the PI controller has better performances, though the fuzzy logic based controller is an intelligent one.

This study presented, the capacities of Multi-Layer Perceptron (MLP) to learn the inverse model of non-linear systems are used to work out the control of a single-phase inverter used as an interface between a

Corresponding Author: A. Ndiaye, Laboratory of Renewable Energy, Polytechnic Higher School, University Cheikh Anta Diop, Dakar-Fann, Senegal

Photovoltaic Generator (PVG) and an electrical grid. The objective is to inject into the grid as much photovoltaic energy as available, with low Total Harmonic Distortion (THD) and good reference signal tracking characteristic.

INVERTER CONTROL BY USING A PI CONTROLLER

The PI controller is the most used controller in industrial systems. It is easy to implement and is cost efficient.

The control scheme of a grid connected photovoltaic system used in this work is given in Fig. 1.

A loop control is elaborated in order to ensure the injection of the maximum available photovoltaic energy into the grid. This loop enables current control given a current reference determined by the maximum power point tracking system (Fig. 1 and 2). In oder to determine the controller parameters, the whole system model has been established. The inverter transfer function links inverter output current to the duty cycle. The PI controller parameters can be determined from this transfer function. The input voltage of the inverter is supposed to be constant (ripple are neglected). From Fig. 1, Eq. (1) can be established:

$$L_{ac}\frac{di_g}{dt} = dV_{dc} - v_g \quad (1)$$

where,
L = Inductor value of the filter
i_g = Current injected into the grid
α = Duty cycle
V_{dc} = Inverter input voltage
v_g = Grid voltage

Using small signals models, it is possible to write:

$$\alpha = \overline{\alpha} + \tilde{\alpha}$$

where,
$\bar{\alpha}$ = The average value of the duty cycle
$\tilde{\alpha}$ = The duty cycle ripple

$$d = \overline{D} + \tilde{d}$$

$$I_g = \bar{I}_g + \tilde{\imath}_g$$

where,
$\bar{I}_g$ = The average value of the current
$\tilde{\imath}_g$ = The current ripple

Considering that the grid average voltage is null and neglecting its ripples, Eq. (2) can be obtained:

$$\frac{d\tilde{i}_g}{dt} = \frac{V_{dc}}{L}\tilde{\alpha} \quad (2)$$

Applying Laplace transform to Eq. (2) and considering the control loop represented in Fig. 2, we get the open loop transfer function expressed by Eq. (3) linking the injected current to the duty cycle:

$$G_g = \left(k_p + \frac{k_i}{s}\right)\frac{G_{ti}}{v_{ti}}\frac{V_{dc}}{sL} \quad (3)$$

where,
v_{it} = The magnitude of the carrier
G_{ti} = Gain loop (gain of the current sensor)

Exploiting this transfer function allows the PI coefficients to be determined Eq. (4) and (5):

$$k_p = \frac{2\pi f_{cL} L v_{ti}}{V_{dc} G_{ti}} \quad (4)$$

$$k_i = \frac{2\pi f_{cL}}{\tan(ph_m)} \quad (5)$$

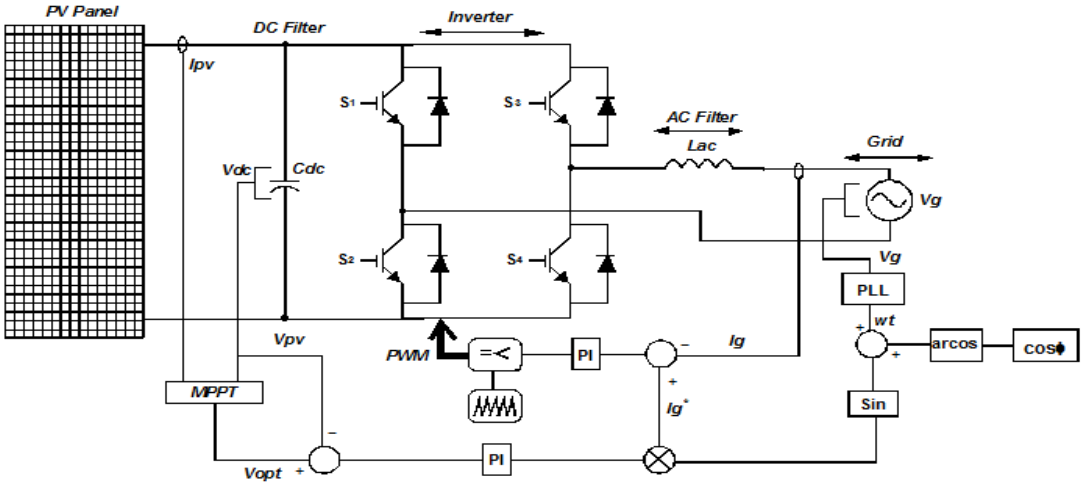

Fig. 1: Control loop of a grid connected photovoltaic system

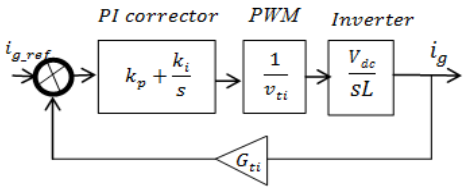

Fig. 2: Control loop of the inverter current

where,
f_{cL} = Cut-off frequency
ph_m = Phase margin

The PI controller input consists of the error between the current provided by the inverter and its reference. The objective of this control is to correct the current injected into the grid (i_g) so that it follows the reference value (i_{gref}).

This type of controllers is simple but it gives limited performances if the system integrates strongly nonlinear elements such as static inverters. In fact, the determination of the controller parameters can be done through different methods but generally depends on the knowledge of the system to be controlled and mathematical model of the system is not always available. Equation (5) and (4) show that the parameters of the PI controller (k_p and k_i) depend on V_{cd} which is related to meteorological conditions (solar irradiation and temperature). So it is worth adapting this coefficient any time the meteorological conditions change, which seems to be impossible. Therefore an adaptive control has to be set up. This fact has led to carrying out a comparative study of a PI corrector and neural network controller.

NEURAL NETWORK CONTROLLER FOR SINGLE PHASE INVERTER

Principles of artificial neural networks: The ANN network is based on models that try to explain human brain functioning. They are adapted to the treatment in parallel of complex problems such as speech and face recognition, or simulation of nonlinear functions. So they offer a new means of information treatment. In Fig. 3, the main elements of an artificial neural are depicted: the input, processing unit and an output.
A formal neuron is characterized by Eq. (6) and (7):

$$x_i = f(A_i) \quad (6)$$

$$A_i = \sum_{j=1}^{N_i} w_{ij} x_i + b_i \quad (7)$$

where,
x_j = State of a neuron j connected to neuron i
A_i = Activity of neuron i
w_{ij} = Weight of the connexion between the neurons j, i
b_i = Bias

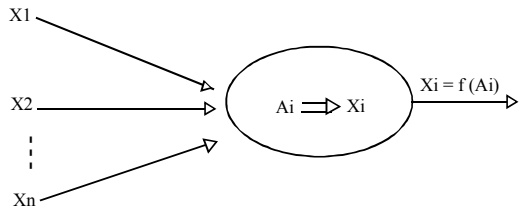

Fig. 3: Representation of a formal neuron

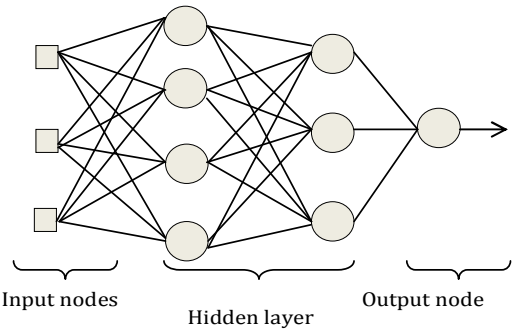

Fig. 4: Architecture of an MLP network

The MLP network (Fig. 4) is a feed forward network that is composed of several layers, each neuron of a layer being totally connected to the neurons of the next layer. The resulting network is able to approximate any nonlinear function.

The error made on the k^{th} output neuron for a sample p is expressed by Eq. (8):

$$\delta p, k = O_{p,k} - x_{p,k} \quad (8)$$

where,
$0_{p,k}$ = Desired output of the neuron k for the sample p
$x_{p,k}$ = Output of the neuron k for the sample p

As a result, the total error (for all output neurons) is estimated by:

$$e_p = \frac{1}{2}\sum_{k=1}^{m} \delta^2{}_{p,k} = \frac{1}{2}\sum_{k=1}^{m}\left(O_{p,k} - x_{p,k}\right)^2$$

where,
m = A number of neurons on the output node

The synaptic weights are then adjusted so as to reduce the output error for the whole samples of the data base:

$$e = \sum_{p=1}^{N} e_p \quad (9)$$

where, N designates the size of the database.

The process of the network parameters estimation is called training. The set of parameters that are to be estimated includes all the weights and biases. An

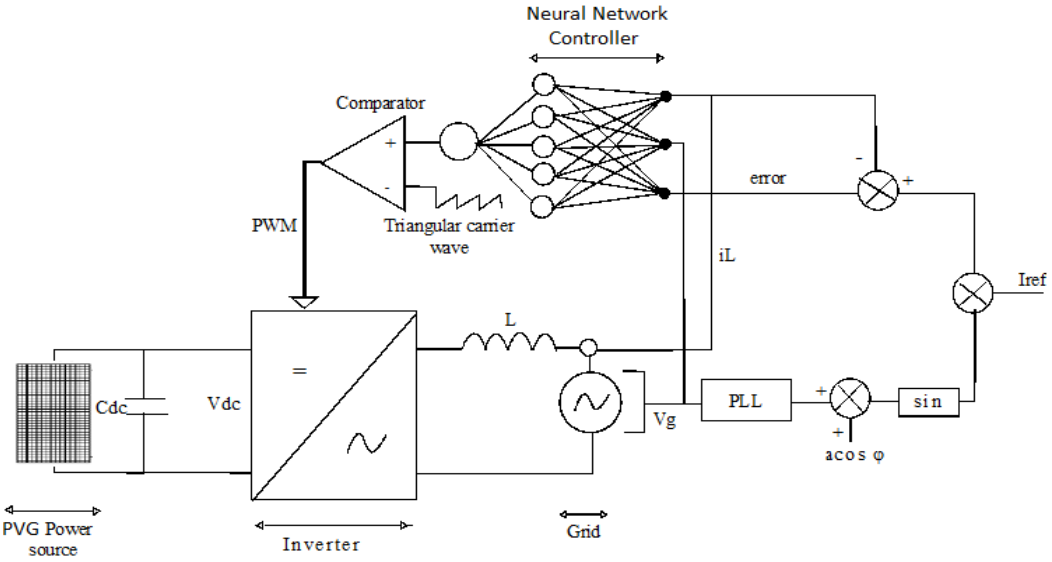

Fig. 5: Grid connected photovoltaic system with single phase inverter and neural controller

algorithm called back propagation is mainly used for the network training. See Ahmed *et al*. (2008) for more details on neural networks.

Proposed design method of the neural controller: Within the framework of this study, the system to control is a single-phase inverter serving as an interface between a photovoltaic generator and an electrical grid. The structure of the neural controller for photovoltaic energy injection into the grid is represented in Fig. 5.

The inputs of the neural controller are the current injected into the grid, the grid voltage and the error between the actual and the reference values of the inverter output current.

Database for the neural controller training is obtainend from the system simulation with several PI controllers, each of witch being determined for a given system operating point, defined by the inverter input DC voltage.

RESULTS AND DISCUSSION

The inverter is designed so that its switches are able to support the maximum current i_{gmax} and the maximum open circuit voltage (V_{co}) of the photovoltaic generator. Table 1 gives the inverter parameters and those of the photovoltaic generator.

The filter inductor value is determined by Eq. (10):

$$L = \frac{V_{dc}}{16\ \Delta I_{max}\ f_s} \quad (10)$$

where,

V_{cd} = The inverter input voltage
fs = The switching frequency
I_{max} = Is the maximum value of the output current ripple

Table 1: Inverter and photovoltaic generator parameters

Parameter	Value
DC bus voltage (Vdc = Vopt at 1 kW/m² and 25°C)	800 V
Opened circuit voltage of the PV generator	1000 V
Short circuit current of the PV generator	6.8 A
Filter inductor value (L)	5 mH
ESR value of the inductor	0.2 Ω
Maximum power of the PV generator	4 kW
Grid RMS voltage value (Vgeff)	220 V
Grid frequency (*fo*)	50 Hz
Inverter switching frequency (*fs*)	20 kHz

Table 2: PI controller parameters

Coefficients	k_p	k_i
Values	5.23	$6.33\ 10^4$

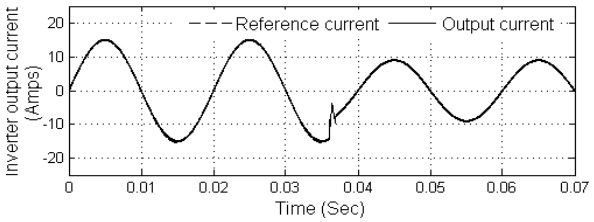

Fig. 6: Inverter output current and its reference value when a PI controller is used

The system is first simulated with the PI controller (Table 2). The injected current and its reference value are presented in Fig. 6, whereas Fig. 7 shows grid voltage and injected current for unity power factor. A disturbance consisting of a 40% reduction of reference current magnitude is introduced at t = 36 ms. The PI controller presents a relatively fast reference current tracking but an important overshoot can be noticed. The main drawbacks of this controller is due to the fact that it has to be designed for a given meteorological conditions.

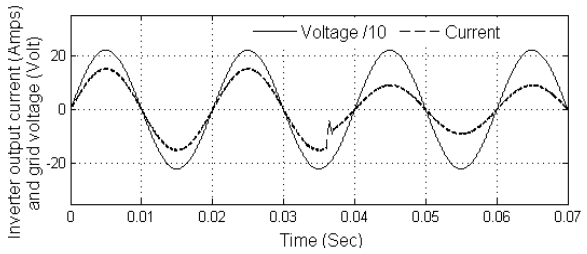

Fig. 7: Grid voltage and inverter output current when a PI controller is used

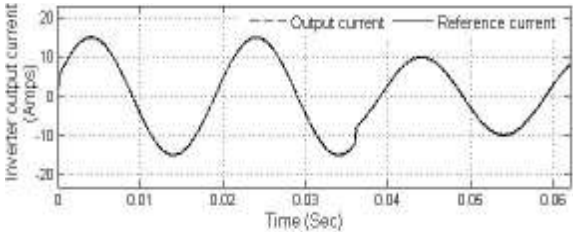

Fig. 8: Inverter output current and its reference value when a neural controller is used

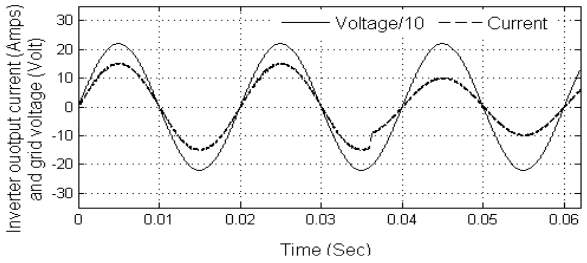

Fig. 9: Grid voltage and inverter output current when a neural controller is used

The design of the neural network controller consists of designing several PI controllers for various meteorological conditions. Following values are used for the solar irradiation and the temperature: (0.25 kW/m², 25°C), (0.25 kW/m², 40°C), (0.6 kW/m², 25°C), (0.6 kW/m², 40°C), (1 kW/m², 25°C) and (1 kW/m², 40°C).

Control signals from the PI controllers, grid voltage, inverter output current and its reference value are gathered to form a large database used for the neural controller training.

Figure 8 shows inverter output current and its reference value when neural controller is used for the following meteorological conditions: a solar irradiation of 1 kW/m² and a temperature of 25°C. A disturbance consisting of a 40% reduction of reference current magnitude is introduced at t = 36 ms. Obtained results prove fast tracking capability of the neural controller without overshoots.

Grid voltage and injected current for unity power factor are shown in Fig. 9.

A comparison study of the two controllers is performed throughout simulation of three cases.

In the first case, the simulation is made for the following meteorological conditions: solar irradiation of 1 kW/m^2 and temperature of 50°C. The PI controller parameters for these meteorological conditions has resulted in $k_p = 1.16$ and $k_i = 7.07\ 10^3$ rad/s.

The Total Harmonic Distortion (THD) of both controllers have been calculated and compared. Obtained results are presented on Fig. 10 and 11. They show that the neuronal controller has a THD slightly weaker than the PI controller.

In the second simulation case, the same meteorological conditions were used but a disturbance

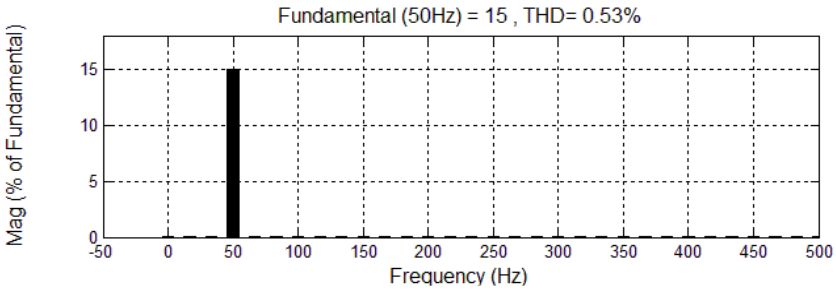

Fig. 10: THD obtained with a PI controller for a solar irradiation of 1 kW/m^2 and a temperature of 50°C

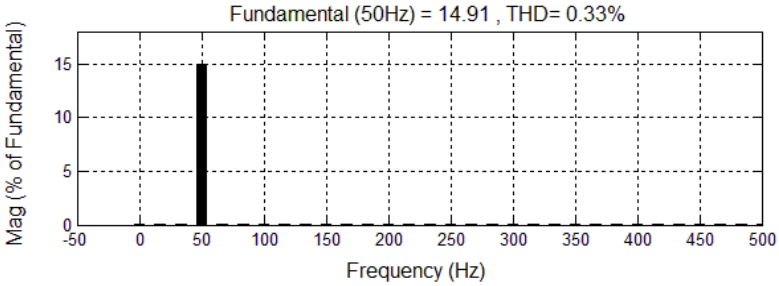

Fig. 11: THD obtained with the neural controller for a solar irradiation of 1 kW/m ^{2} and a temperature of 50°C

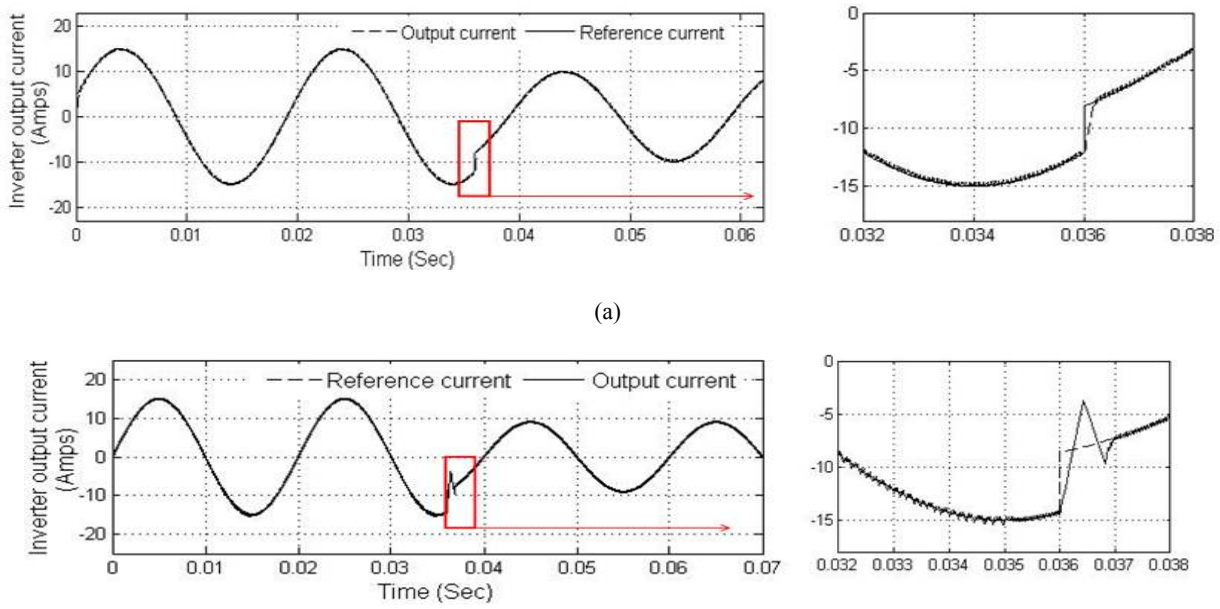

Fig. 12: Performances of the neuronal controller, (a) and PI controller of (b) with disturbance, for an irradiation of 1 kW/m^2 and a temperature of 50°C

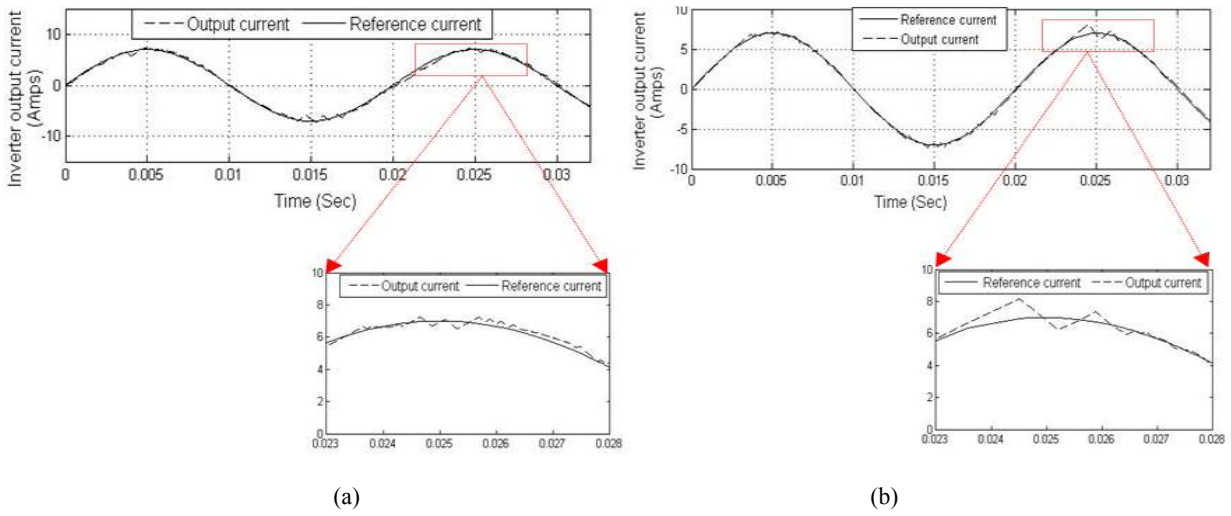

Fig. 13: Current injected for a solar irradiation of 0.172 kW/m^2 and a temperature of 25°C: (a) neural controller, (b) IP controller

Table 3: Comparison results of the PI and neural controller

Performance	Neural controller	PI controller
Time response (ms)	0.50	1
Overshoot current (A)	0	5
Total Harmonic Distortion (THD) (%)	0.33	0.53
Magnitude of the fundamental current (A)	14.96	15
Relative current error: 100* (i_g - i_{g_ref}) /$_{Ig\_refmax}$	0.67	1.33

consisting in a rapid variation of the reference current has been introduced. The simulation results are represented on Fig. 12 and in Table 3. These results show that the relative error between the injected current and its reference is weaker for the neural controller, be it the half of the one obtained by PI controller. Moreover, the PI controller has a response time twice greater than that of the neural controller. Unlike the PI controller, the neural controller responds to the disturbance without overshoot. These two controllers provide a fundamental magnitude of about 15 A. Yet, considering the nature of both signals, the neural controller gets closer to the reference, giving its weak THD (Fig. 10 and 11).

In the third case of simulation the following values of the solar irradiation and temperature were used: G = 0.172 kW/m^2 and T = 25°C; but the PI correct

calculated for a solar irradiation of 1 kW/m² and a temperature of 50°C is maintained. Figure 13 gives the simulation results. The latter show that when the meteorology conditions change meaningfully, the PI corrector performances decrease. On the other hand the neural controller adapts itself well to the variations of the meteorological conditions.

In Sajedi *et al*. (2011), Hoseynpoor and Pirzadeh Ashraf (2011) controlled the current injected in network by the method "Adaptive Predictive Current Control (APCC)" presents a THD of 2.5% for an irradiation of 1 kW/m^2. With the same irradiation, we have been able to get a THD of about 3.7 times smaller.

CONCLUSION

A neural controller and a PI controller were presented in this study in a purpose of a grid connected photovoltaic power system. The training and validation data of the used neural controller were obtained by simulation of the whole system with several PI controllers calculated for various meteorological conditions. The simulation results show that the neural controller gives better results than a PI controller. The advantage of neural network based controller is that it adapts to the changing of meteorological conditions unlike the IP controller whose performance decreases during a strong variation of the temperature and/or irradiation.

REFERENCES

Ahmed, T., A. Hamza, A. Abdel Ghani, 2008. La commande neuronale de la machine à réluctance variable. Rev. Roum. Sci. Techn.-Électrotechn. et Énerg., 53(4): 473-482.

Branštetter, P. and M. Skotnica, 2000. Application of artificial neural network for speed control of asynchronous motor with vector control. Proceedings of International Conference of Košice, EPE-PEMC, pp: 6-157-6-159.

Cybenko, G., 1989. Approximation by superposition of a sigmoidal function. Math. Control Signals Syst., 2: 303-314.

Dreyfus, G., 2002. Neural Networks: Methodologies and Applications. Eyrolles Press.

Hoseynpoor, Y. and T. Pirzadeh Ashraf, 2011. Maximum power point tracking and reactive power control of single stage grid connected photovoltaic system. Res. J. Appl. Sci., Eng. Technol., 3(12): 1430-1436.

Mohammed, S., E.C. Djamel and M. Fayçal Khelfi, 2007. Commande neuronale inverse des systèmes nonlinéaires. Proceeding of the 4th International Conference on Computer Integrated Manufacturing (CIP'2007). November 03-04.

Panos, J.A. and M.P. Kevin, 1993. Introduction to Intelligent and Autonomous Control. Kluwer Academic Publishers, ISBN: 0-7923-9267-1.

Rivals, I., L. Personnaz, G. Dreyfus and J.L. Ploix, 1995. Modélisation, Classification et Commande par Réseaux de Neurones: Principes Fondamentaux, Méthodologie de Conception et Illustrations Industrielles. In: Corriou, J.P. (Ed.), Les réseaux de Neurones pour la Modélisation et la Commande de Procédés (Lavoisier Tec et Doc, 1995), pp: 1-37.

Ronco, E. and P.J. Gawthrop, 1997. Neural networks for modelling and control. Techncal Report CSC-97008, Center for Systems and Control, Glasgow.

Sajedi, S., F. Khalifeh, Z. Khalifeh and T. Karimi, 2011. Investigation of a new control structure of grid connected single stage PV system. J. Basic Appl. Sci. Res., 1(12): 2543 2551.

Tine, V., R. Bert, D.B. Frederik, M. Bart and V. Lieven, 2009. A voltage-source inverter for microgrid applications with an inner current control loop and an outer voltage control loop. Proceeding of the International Conference on Renewable Energies and Power Quality (ICREPQ09). Valencia (Spain), April 15th-17th.

Wishart, M.T. and R.G. Harley, 1995. Identification and control of induction machines using artificial neural networks. IEEE T. Ind. Appl., 31(3).

Yildirim, S., 1997. New neural networks for adaptive control of robot manipulators. Proceeding of International Conference on Neural Networks, 3: 1727-1731.